Original Article

Available online at
www.heca-analitika.com/ijcr

Indonesian Journal of Case Reports

Vol. 2, No. 2, 2024

Enhancing Early Detection of Alzheimer's Disease through MRI using Explainable Artificial Intelligence

Teuku Rizky Noviandy [1], Ghifari Maulana Idroes [2], Adi Purnawarman [3], Imran Imran [4], Nova Dian Lestari [4], Sri Hastuti [5] and Rinaldi Idroes [6,*]

1 Department of Information Systems, Faculty of Engineering, Universitas Abulyatama, Aceh Besar 23372, Indonesia; rizky_si@abulyatama.ac.id (T.R.N.)
2 Department of Nuclear Engineering and Engineering Physics, Universitas Gadjah Mada, Yogyakarta 55281, Indonesia; ghifarimaulanaidroes@mail.ugm.ac.id
3 Department of Cardiology and Vascular Medicine, Faculty of Medicine, Universitas Syiah Kuala, Banda Aceh 23111, Indonesia; adilbfk@usk.ac.id (A.P.)
4 Department of Neurology, Faculty of Medicine, Universitas Syiah Kuala, Banda Aceh 23111, Indonesia; imran@usk.ac.id (I.I.); novadianlestari@usk.ac.id (N.D.L.)
5 Department of Neurology, General Hospital dr. Zainoel Abidin, Banda Aceh, 23111, Indonesia; wiwid.srihastuti@gmail.com (S.H.)
6 School of Mathematics and Applied Sciences, Universitas Syiah Kuala, Banda Aceh 23111, Indonesia; rinaldi.idroes@usk.ac.id (R.I.)

* Correspondence: rinaldi.idroes@usk.ac.id

Article History

Received 5 October 2024
Revised 6 December 2024
Accepted 13 December 2024
Available Online 21 December 2024

Keywords:
Deep learning
Grad-CAM
ResNet50

Abstract

Alzheimer's disease is a progressive brain disorder that causes memory loss and cognitive decline, affecting millions of people worldwide. Early detection is critical for slowing the disease's progression and improving patient outcomes. Magnetic Resonance Imaging (MRI) is widely used to identify brain changes associated with AD, but subtle abnormalities in the early stages are often difficult to detect using traditional methods. In this study, we used a deep learning approach with a model called ResNet-50 to analyze MRI scans and classify patients into four categories: Non-Demented, Very Mild Demented, Mild Demented, and Moderate Demented. The model was trained using MRI images, achieving an accuracy of 95.63%, with strong sensitivity, precision, and specificity. To make the model's predictions understandable for healthcare professionals, we applied a technique called Grad-CAM, which highlights areas of the brain that influenced the model's decisions. These visual explanations help clinicians see and trust the reasoning behind the AI's results. While the model performed well overall, misclassifications between adjacent disease stages were observed, likely due to class imbalance and subtle brain changes. This study demonstrates that explainable AI tools can improve early detection of Alzheimer's disease, supporting clinicians in making accurate and timely diagnoses. Future work will focus on expanding the dataset and combining MRI with other clinical information to enhance the tool's reliability in real-world settings.

1. Introduction

Alzheimer's disease is a progressive neurodegenerative disorder characterized by cognitive decline, memory loss, and behavioral changes [1, 2]. It is the most common cause of dementia, affecting 50 million individuals globally [3, 4]. As the disease progresses, it severely impacts the quality of life of patients and places significant emotional and financial strain on caregivers and healthcare systems [5–7]. Early detection of

Alzheimer's disease is important because it allows for timely interventions, such as initiating medications to slow cognitive decline, implementing lifestyle changes to preserve brain function, and providing patients and caregivers with resources for planning and support.

Current methods for detecting Alzheimer's disease rely heavily on medical imaging techniques such as Magnetic Resonance Imaging (MRI) [8]. MRI scans identify structural brain abnormalities, such as atrophy in specific regions associated with the disease. However, conventional analysis of MRI images often requires highly specialized expertise and significant time, making early detection challenging in clinical practice. Moreover, subtle changes in the brain can be difficult to identify in the early stages of the disease.

With the rapid advancements in Artificial Intelligence (AI), particularly in the domains of deep learning and machine learning, the potential to revolutionize Alzheimer's disease detection has significantly increased [9, 10]. AI refers to machines' simulation of human intelligence, encompassing the ability to process information, learn from data, and make decisions [11, 12]. Deep learning is a key subset of AI, which involves neural networks capable of automatically extracting and learning complex patterns from large datasets [13]. Deep learning models are especially well-suited for analyzing medical imaging data, enabling the identification of intricate patterns and biomarkers that may not be readily apparent to human experts. These capabilities allow for faster and potentially more accurate detection of Alzheimer's disease, even in its earliest stages. Importantly, AI does not aim to replace doctors but rather to assist them by providing powerful tools that enhance their ability to diagnose and treat patients efficiently.

Recent studies have utilized deep learning techniques for the early detection and classification of AD, leveraging MRI brain imaging for diagnosis. Orouskhani et al. [14] proposed a novel deep triplet network inspired by VGG16, employing a conditional loss function to address limited sample availability and improve accuracy, outperforming state-of-the-art models on the OASIS dataset. Salehi et al. [15] implemented a Convolutional Neural Network (CNN) for classifying Alzheimer's disease using the ADNI dataset, achieving an impressive 99% accuracy, highlighting the superiority of deep learning over traditional machine learning for large medical datasets. Similarly, Saratxaga et al. [16] developed a deep learning-based method achieving a balanced accuracy of up to 0.93 for automated diagnosis and disease staging using the OASIS dataset, surpassing previous approaches and demonstrating the robustness of deep learning in Alzheimer's disease diagnosis.

However, despite these promising advancements, many AI systems operate in ways that can be difficult to interpret or explain [17]. This lack of transparency poses challenges for clinical adoption, as healthcare professionals need to trust and understand the reasoning behind AI-generated predictions. To address these challenges, Explainable Artificial Intelligence (XAI) has emerged as an important field [18]. XAI focuses on creating systems that provide clear, interpretable, and actionable insights into how decisions are made. This transparency is vital in medical applications, where clinicians and patients must understand the rationale behind diagnoses and predictions. By offering interpretable and trustworthy AI tools, XAI bridges the gap between advanced computational models and clinical practice, ensuring trust, informed decision-making, and improved healthcare outcomes in Alzheimer's detection.

This study aims to improve early detection of Alzheimer's disease by using XAI methods applied to MRI data. The goal is to create an AI system that is not only accurate but also easy for healthcare professionals to interpret and apply in their practice. By focusing on transparency and usability, the study seeks to make advanced computational tools more practical and reliable for clinical use. This approach is expected to support early diagnosis of Alzheimer's disease, provide clearer insights into its progression, and help develop more personalized and effective treatment strategies for patients.

2. Materials and Methods

2.1. Dataset

The dataset used in this study was retrieved from the Mendeley Data repository, published by Yakkundi [19]. It is divided into four classes: Non-Demented, Very Mildly Demented, Mildly Demented, and Moderately Demented. This dataset was chosen due to its clear categorization and publicly available, ensuring accessibility and comparability. The distribution can be seen in Table 1, and an overview of the MRI images for each class is shown in Figure 1.

To prepare the dataset for the study, the MRI images were resized to 224 by 224 pixels to ensure uniformity in input dimensions for the AI models. The images were then normalized to scale pixel values to a range of zero to one, a standard preprocessing step to improve the performance and convergence of deep learning algorithms.

The dataset was subsequently split into three subsets: 70% for training, 20% for validation, and 10% for testing. This resulted in 4,480 images for training, 1,280 images

Table 1. Distribution of the early Alzheimer's disease MRI dataset

Class	Number of Samples
Non-Demented	3,200
Very Mild Demented	2,240
Mild Demented	896
Moderate Demented	64

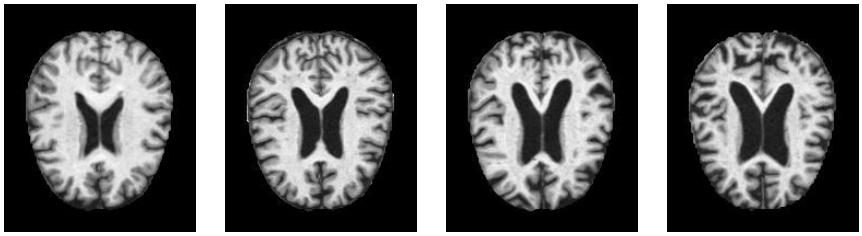

Figure 1. Representative MRI images for each class, (a) Non-Demented, (b) Very Mild Demented, (c) Mild Demented, and (d) Moderate Demented.

Table 2. Training parameters summary.

Parameter	Value
Loss Function	Cross-Entropy Loss
Optimizer	Adam
Learning Rate	0.0001
Weight Decay	1.00×10^{-6}
Maximum Epochs	100
Early Stopping Patience	10 epochs

for validation, and 640 images for testing. The training set was used to train the deep learning models, the validation set was utilized for hyperparameter tuning and monitoring training performance, and the testing set was reserved exclusively for evaluating the final model's performance. To ensure unbiased evaluation, samples in the testing set were excluded from the training and validation sets.

2.2. Deep Learning Model

This study used ResNet-50, a popular deep-learning model well-suited for image classification tasks [20]. ResNet-50, short for Residual Network with 50 layers, is a type of CNN designed to process and analyze visual data like images. What makes ResNet-50 particularly effective is its use of "residual connections." These connections allow the model to skip certain layers during processing, which helps it learn more efficiently and prevents performance issues that often arise as networks become deeper and more complex. In this study, ResNet-50 was specifically chosen for its ability to extract meaningful features from images, making it ideal for detecting the subtle patterns in MRI scans required for early Alzheimer's diagnosis. Compared to other models, it offers an excellent balance between depth, computational efficiency, and accuracy, which is crucial for effectively handling high-dimensional medical imaging data.

To adapt ResNet-50 for our task of classifying MRI images, we customized the model to focus on our specific needs. First, we used a pre-trained version of ResNet-50 that had already learned general image features from a large and diverse dataset. This technique, called transfer learning, allows us to benefit from the model's prior knowledge, enabling faster training and better performance with a relatively small dataset.

Next, we optimized the model by freezing the early layers responsible for detecting basic image features such as edges and textures. These layers do not need retraining, as they are already well-suited for general image processing. Only the final block of layers, which specializes in more task-specific patterns, was left trainable. Additionally, the original fully connected output layer of ResNet-50 was replaced with a custom output layer tailored to classify the images into the four required categories. This new layer included a dropout mechanism to prevent overfitting and a dense layer to output predictions for the classes. The training process used the parameters summarized in Table 2.

During training, the loss function used was cross-entropy loss, which measures the difference between the predicted and actual class labels and helps guide the model to improve its predictions. The Adam optimizer was employed to adjust the model's parameters based on the loss, with a learning rate set to 0.0001 and a small weight decay to reduce overfitting.

The training process was carried out over a maximum of 100 epochs, but early stopping was implemented to monitor the model's performance on the validation

dataset. Early stopping ensures that the training stops automatically if the model does not improve for ten consecutive epochs. This avoids overtraining and saves computational resources. Additionally, the best-performing model based on validation accuracy was saved at the end of each epoch. Once the training was complete, this saved model was loaded for final evaluation on the test dataset. This carefully designed process ensured the ResNet-50 model was accurate, efficient, and robust for detecting Alzheimer's disease from MRI scans.

2.3. Evaluation of Model Performance

The model's performance was evaluated using five key metrics: accuracy, precision, sensitivity, specificity, and F1-score [21]. Since this study involves multiclass classification, all metrics were calculated using a weighted average to account for the class imbalance in the dataset [22]. In a weighted average, the contribution of each class to the overall metric is proportional to the number of samples in that class. This approach ensures that metrics for smaller classes, such as Moderate Demented, are not overshadowed by metrics for larger classes.

Accuracy represents the proportion of correctly classified samples across all classes. It is calculated as the ratio of the sum of true positives and true negatives to the total number of samples. Precision measures the proportion of correctly predicted positive samples among all samples predicted as positive for each class, weighted by the number of samples in each class. Sensitivity, also known as recall, calculates the proportion of true positive predictions out of the actual positive samples for each class, again weighted by class size. Specificity quantifies the ability to correctly identify negative samples, reflecting how well the model avoids false positives. Finally, the F1-score combines precision and sensitivity into a single metric by calculating their harmonic mean, providing a balance between these two measures. The formulas for each metric are shown in Equation 1-5, respectively:

$$Accuracy = \frac{TP + TN}{TP + TN + FP + FN} \quad (1)$$

$$Precision = \sum_{i=1}^{N} w_i \frac{TP_i}{TP_i + FP_i} \quad (2)$$

$$Sensitivity = \sum_{i=1}^{N} w_i \frac{TP_i}{TP_i + FN_i} \quad (3)$$

$$Specificity = \sum_{i=1}^{N} w_i \frac{TN_i}{TN_i + FP_i} \quad (4)$$

$$F1 - Score = \sum_{i=1}^{N} w_i \frac{2 \times Precision_i \times Sensitivity_i}{Precision_i + Sensitivity_i} \quad (5)$$

where N represents the total number of classes, w_i the weight of each class calculated as the proportion of samples in that class, and TP_i, TN_i, FP_i, FN_i refer to the true positives, true negatives, false positives, and false negatives for class i, respectively.

2.4. Explainable Artificial Intelligence

We used Gradient-weighted Class Activation Mapping (Grad-CAM) to make the deep learning model interpretable. Grad-CAM is commonly applied in medical imaging to provide visual explanations for CNNs predictions. It highlights the regions of an input image that contribute most to the model's decision, helping researchers and clinicians understand the basis of the AI's outputs [23].

Grad-CAM works by using the gradients of the target class with respect to the final convolutional layer of the model. These gradients are used to calculate weights for the layer's feature maps. A heatmap is then generated by combining the feature maps with these weights, showing the areas of the brain MRI that influenced the model's classification [24].

In this study, Grad-CAM was applied to the predictions of the ResNet-50 model. The resulting heatmaps were examined to verify that the highlighted regions corresponded to relevant anatomical structures. This approach ensures that the model's predictions are accurate and interpretable, making it a practical tool for clinical use [25, 26].

3. Results and Discussion

The model was trained for 35 epochs, and early stopping was implemented to monitor validation loss. Early stopping was triggered at epoch 35 as the validation loss showed no significant improvement, ensuring that the model stopped training at an optimal point to avoid overfitting.

The training and validation loss curves over the 35 epochs are shown in Figure 2. The training loss decreases consistently and stabilizes near zero, indicating effective learning on the training dataset. In contrast, the validation loss drops sharply during the initial epochs, reflecting rapid learning and generalization. However, as training progresses, the validation loss begins to fluctuate, signaling that the model starts to overfit slightly to the training data. Despite this fluctuation, the validation loss remains relatively low due to the early

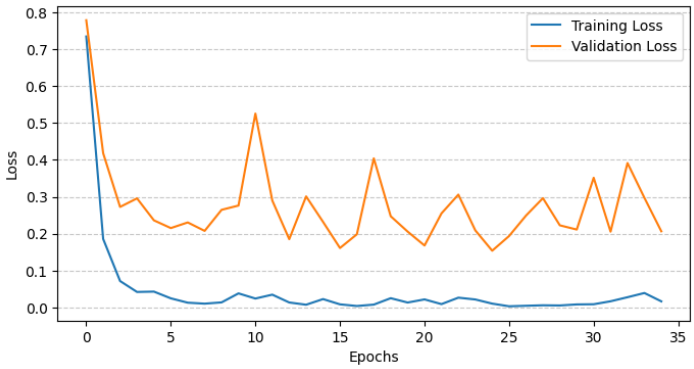

Figure 2. Training and validation loss curves over 35 epochs.

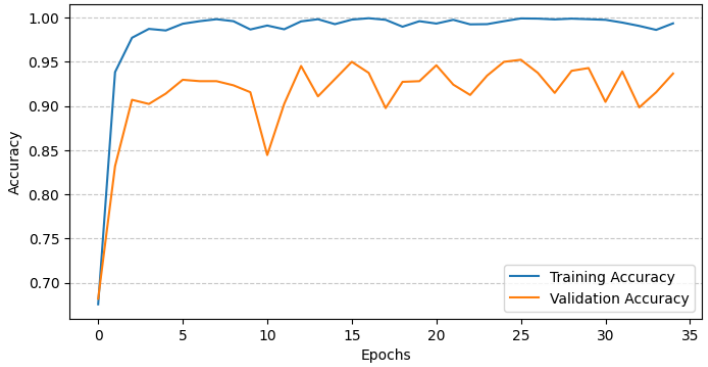

Figure 3. Training and validation accuracy curves over 35 epochs.

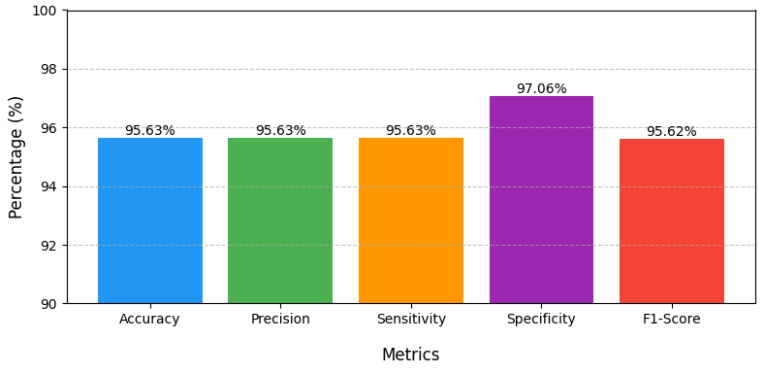

Figure 4. Performance metrics of the ResNet-50 model for Alzheimer's disease detection.

stopping mechanism, which prevents further degradation of generalization performance.

The training and validation accuracy curves are displayed in Figure 3. The training accuracy rises steeply during the first few epochs and stabilizes around 99%, showing that the model successfully learns the patterns within the training data. The validation accuracy increases sharply in the early stages and stabilizes between 90% and 95%, suggesting strong generalization on unseen data. The fluctuations observed in validation accuracy, especially in later epochs, align with the trends seen in the validation loss. This behavior indicates the model performs well overall but exhibits minor instability due to the relatively small validation set size or the class imbalance present in the dataset.

The performance of the model was evaluated using accuracy, precision, sensitivity, specificity, and F1-score, as shown in Figure 4. The model achieved an accuracy, precision, and sensitivity of 95.63%, indicating consistent performance across different metrics. The slightly higher specificity of 97.06% reflects the model's strong ability to correctly identify negative samples, which is particularly important in medical applications to avoid false positives. The F1-score, which balances precision and sensitivity, was 95.62%, demonstrating the model's robust overall performance despite class imbalance.

Figure 5 shows the confusion matrix for the model's predictions. It provides a breakdown of correctly and incorrectly classified samples across the four classes: Non-Demented, Very Mild Demented, Mild Demented,

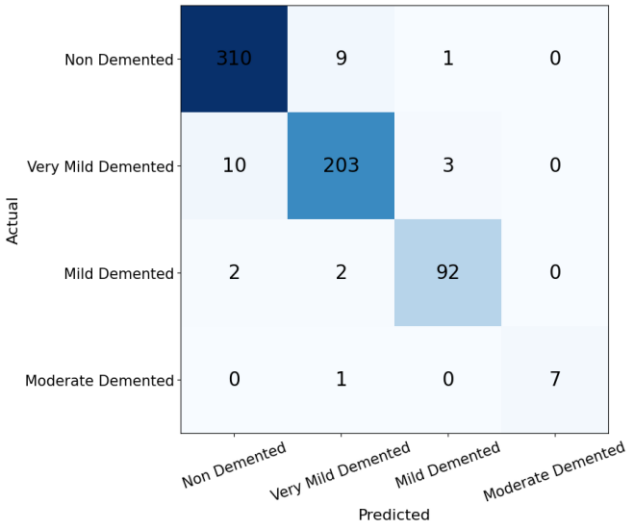

Figure 5. Confusion matrix of the ResNet-50 model predictions for Alzheimer's disease classification.

and Moderate Demented. The results show that the model performs well overall but struggles with misclassifications between adjacent stages of Alzheimer's disease.

The model correctly classified 310 out of 320 samples for the Non-Demented class. However, 9 samples were misclassified as Very Mild Demented, and 1 sample as Mild Demented. These errors likely stem from subtle structural changes in brain MRI images that overlap with the early stages of dementia. Such overlaps can make distinguishing between healthy individuals and those in the very early stages of the disease challenging, even for advanced AI models.

In the Very Mild Demented class, the model correctly classified 203 out of 216 samples, but 10 were incorrectly labeled as Non-Demented and 3 as Mild Demented. The misclassification between Very Mild Demented and Non-Demented may be due to the subtle progression of brain changes in the early stages of Alzheimer's, where some features still resemble those of healthy individuals. Similarly, errors between Very Mild and Mild Demented classes occur because these stages share overlapping characteristics, making it difficult for the model to draw clear boundaries.

For the Mild Demented class, the model achieved 92 correct predictions out of 96 samples, but 2 samples were misclassified as Non-Demented and another two samples as Very Mild Demented. These errors may be caused by the gradual nature of brain atrophy, where the structural differences between adjacent stages are not distinct enough in some cases. Misclassifications in this class highlight the challenge of distinguishing Mild Demented from both earlier and non-demented stages.

In the Moderate Demented class, the model correctly classified 7 out of 8 samples, with 1 sample being misclassified as Very Mild Demented. The small size of this class, with only 8 samples available, likely contributed to the misclassification. With limited data, the model may struggle to generalize and learn the specific features of the Moderate Demented stage effectively. This highlights the impact of class imbalance on model performance, especially for underrepresented stages.

The misclassifications observed in the confusion matrix predominantly occur between adjacent stages of Alzheimer's disease, such as Non-Demented and Very Mild Demented or Very Mild Demented and Mild Demented. These errors are expected because Alzheimer's progression is gradual, with overlapping features between neighboring stages. Additionally, the small sample size for the Moderate Demented class affects the model's ability to recognize its distinct features.

Figure 6 presents Grad-CAM visualizations for predictions made by the ResNet-50 model. The top row displays the original MRI images from different classes: Non-Demented, Very Mild Demented, Mild Demented, and Moderate Demented. The bottom row shows the corresponding Grad-CAM heatmaps, highlighting the brain regions that influenced the model's predictions.

In the Non-Demented case, the Grad-CAM heatmap shows minimal activation in regions typically associated with Alzheimer's disease, aligning with the absence of structural abnormalities. For the Very Mild Demented class, the highlighted areas show subtle activation regions, indicating the model's focus on potential early signs of brain atrophy. In the Mild Demented case, the activation becomes more pronounced in specific brain regions, such as the hippocampus and surrounding

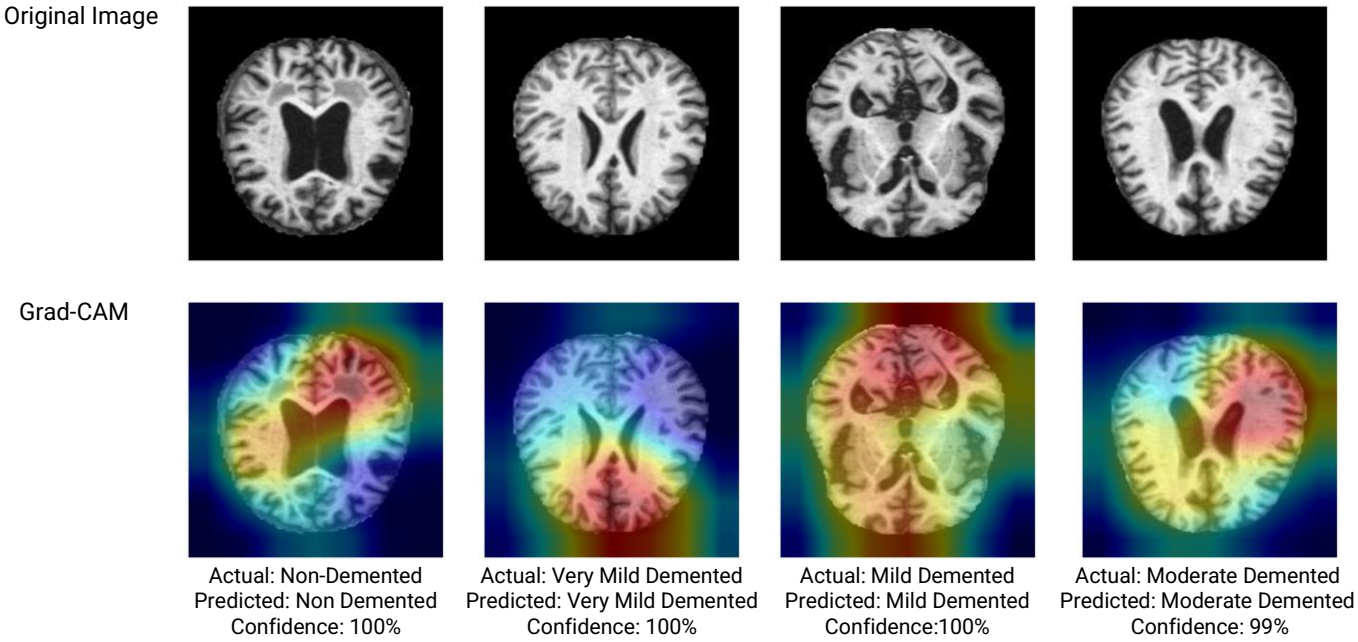

Figure 6. Grad-CAM visualizations of ResNet-50 predictions for Non-Demented, Very Mild Demented, Mild Demented, and Moderate Demented classes. The heatmaps highlight regions in the brain that contributed most to the model's decision.

areas, commonly associated with Alzheimer's progression. For the Moderate Demented class, the Grad-CAM heatmap highlights extensive regions of the brain, reflecting more advanced structural changes typically seen at this stage of the disease.

The high confidence predictions across all four cases demonstrate the model's ability to identify and focus on relevant regions of interest within the MRI scans. The Grad-CAM visualizations validate the correctness of the model's predictions and provide a transparent explanation of its decision-making process. These insights are critical for clinical applications, as they help healthcare professionals interpret and trust the AI's outputs.

The findings of this study demonstrate the potential of deep learning models, specifically ResNet-50, in the early detection and classification of Alzheimer's disease using MRI data. The high accuracy, precision, and sensitivity observed suggest that the model is capable of identifying subtle structural brain changes across different stages of the disease. This has significant clinical implications, as accurate and early detection can enable timely interventions, personalized treatment planning, and improved management of the disease. Furthermore, using Grad-CAM visualizations ensures interpretability, helping healthcare professionals trust the model's decisions by providing insights into the brain regions that influenced predictions. This interpretability is particularly important for building confidence in AI-based diagnostic tools in real-world clinical settings.

The study has several limitations that should be addressed in future work. One significant issue is the class imbalance in the dataset, particularly for the Moderate Demented category, which had far fewer samples than other classes. This imbalance likely impacted the model's ability to generalize well for this underrepresented stage, resulting in occasional misclassifications. To mitigate this, increasing the number of Moderate Demented samples or using data augmentation to expand the dataset artificially would be beneficial. Additionally, the study relied solely on MRI data for classification. While MRI provides valuable structural information, Alzheimer's disease involves various factors. Incorporating additional data types, such as cognitive test scores, genetic markers, or functional imaging, could improve the model's ability to distinguish between adjacent stages of the disease and enhance its overall performance.

Another limitation was minor fluctuations in validation loss and accuracy during training, which suggest slight overfitting despite the use of early stopping. Addressing this could involve exploring regularization techniques like adjusting dropout rates or employing advanced optimization methods to improve generalization. Expanding the dataset by including images from diverse sources and demographics would further validate the model's robustness. Future work should also focus on

expanding the dataset for later stages of Alzheimer's disease and incorporating longitudinal MRI data to enable the prediction of disease progression over time. Exploring advanced architectures like transformers, multi-modal frameworks, or ensemble models may enhance performance. Lastly, clinical validation using real-world patient data will be critical to evaluate the model's practical application in healthcare settings.

4. Conclusions

This study demonstrated the effectiveness of the ResNet-50 deep learning model for the early detection and classification of Alzheimer's disease using MRI data. The model achieved an accuracy of 95.63%, precision of 95.63%, sensitivity of 95.63%, specificity of 97.06%, and an F1-score of 95.62%, indicating strong and consistent performance across all evaluation metrics. Grad-CAM visualizations provided interpretability by highlighting key brain regions influencing the model's predictions, ensuring transparency and clinical relevance. While challenges such as class imbalance, particularly in the Moderate Demented class, the results highlight the model's potential for real-world clinical applications. Future work should address class imbalance, incorporate multi-modal data, and validate the model on larger and more diverse datasets to improve robustness and generalizability.

Author Contributions: Conceptualization, T.R.N. and R.I.; methodology, T.R.N., I.I., N.D.L. and R.I.; software, T.R.N. and G.M.I.; validation, I.I., S.H. and R.I.; formal analysis, T.R.N., A.P., and S.H.; investigation, T.R.N., A.P., and S.H.; resources, I.I., N.D.L., and S.H.; data curation, I.I., N.D.L. and S.H.; writing—original draft preparation, T.R.N., G.M.I. and A.P.; writing—review and editing, I.I., N.D.L., S.H., and R.I.; visualization, T.R.N. and G.M.I.; supervision, R.I.; project administration, R.I.; funding acquisition, R.I. All authors have read and agreed to the published version of the manuscript.

Funding: This study does not receive external funding.

Ethical Clearance: Not applicable.

Informed Consent Statement: Not applicable.

Data Availability Statement: The dataset can be accessed at https://data.mendeley.com/datasets/ch87yswbz4/1.

Conflicts of Interest: All the authors declare that there are no conflicts of interest.

References

1. Yiannopoulou, K. G., and Papageorgiou, S. G. (2020). Current and Future Treatments in Alzheimer Disease: An Update, *Journal of Central Nervous System Disease*, Vol. 12, 117957352090739. doi:10.1177/1179573520907397.
2. Sen, S., Meur, S., Nandi, G., and Karati, D. (2024). Unlocking the Potential: Woodfordia fruticosa Kurz in Alzheimer's Disease Management – a Concise Review, *Brain Disorders*, Vol. 16, 100171. doi:10.1016/j.dscb.2024.100171.
3. Gholami, A. (2023). Alzheimer's Disease: The Role of Proteins in Formation, Mechanisms, and New Therapeutic Approaches, *Neuroscience Letters*, Vol. 817, 137532. doi:10.1016/j.neulet.2023.137532.
4. Chaudhary, R. K., Mateti, U. V., Khanal, P., Rawal, K. B., Jain, P., Patil, V. S., Shrivastava, A. K., and Patil, B. M. (2024). Alzheimer's Disease: Epidemiology, Neuropathology, and Neurochemistry, *Computational and Experimental Studies in Alzheimer's Disease*, CRC Press, 1–14.
5. Kang, Y., Yeap, Y. J., Yang, J., Ma, S., Lim, K. L., Zhang, Q., Lu, L., and Zhang, C. (2024). Role of Lipid Droplets in Neurodegenerative Diseases: From Pathogenesis to Therapeutics, *Neuroscience & Biobehavioral Reviews*, Vol. 165, 105867. doi:10.1016/j.neubiorev.2024.105867.
6. Xu, L. (2023). The Multifaceted Pressures Faced by Family Caregivers of Alzheimer's Disease, *Journal of Education, Humanities and Social Sciences*, Vol. 24, 379–384. doi:10.54097/yrvywn95.
7. Felekoğlu, E., Özalevli, S., Yakut, H., Aktan, R., and Yener, G. (2021). Investigation of the Factors Affecting Quality of Life in Patients with Mild to Moderate Alzheimer's Disease in Terms of Patients and Caregivers, *Medicina*, Vol. 57, No. 10, 1067. doi:10.3390/medicina57101067.
8. Henry-Feugeas, M. C. (2007). MRI of the 'Alzheimer Syndrome', *Journal of Neuroradiology*, Vol. 34, No. 4, 220–227. doi:10.1016/j.neurad.2007.07.002.
9. Noviandy, T. R., Nisa, K., Idroes, G. M., Hardi, I., and Sasmita, N. R. (2024). Classifying Beta-Secretase 1 Inhibitor Activity for Alzheimer's Drug Discovery with LightGBM, Journal of Computing Theories and Applications, Vol. 2, No. 2, 138–147. doi:10.62411/jcta.10129.
10. Haug, C. J., and Drazen, J. M. (2023). Artificial Intelligence and Machine Learning in Clinical Medicine, 2023, *New England Journal of Medicine*, Vol. 388, No. 13, 1201–1208. doi:10.1056/NEJMra2302038.
11. Noviandy, T. R., Maulana, A., Idroes, G. M., Suhendra, R., Afidh, R. P. F., and Idroes, R. (2024). An Explainable Multi-Model Stacked Classifier Approach for Predicting Hepatitis C Drug Candidates, *Sci*, Vol. 6, No. 4, 81. doi:10.3390/sci6040081.
12. Noviandy, T. R., Maulana, A., Emran, T. B., Idroes, G. M., and Idroes, R. (2023). QSAR Classification of Beta-Secretase 1 Inhibitor Activity in Alzheimer's Disease Using Ensemble Machine Learning Algorithms, *Heca Journal of Applied Sciences*, Vol. 1, No. 1, 1–7. doi:10.60084/hjas.v1i1.12.
13. Kaul, V., Enslin, S., and Gross, S. A. (2020). History of Artificial Intelligence in Medicine, *Gastrointestinal Endoscopy*, Vol. 92, No. 4, 807–812. doi:10.1016/j.gie.2020.06.040.
14. Orouskhani, M., Zhu, C., Rostamian, S., Shomal Zadeh, F., Shafiei, M., and Orouskhani, Y. (2022). Alzheimer's Disease Detection from Structural MRI Using Conditional Deep Triplet Network, *Neuroscience Informatics*, Vol. 2, No. 4, 100066. doi:10.1016/j.neuri.2022.100066.
15. Salehi, A. W., Baglat, P., Sharma, B. B., Gupta, G., and Upadhya, A. (2020). A CNN Model: Earlier Diagnosis and Classification of Alzheimer Disease using MRI, *2020 International Conference on Smart Electronics and Communication (ICOSEC)*, IEEE, 156–161. doi:10.1109/ICOSEC49089.2020.9215402.
16. Saratxaga, C. L., Moya, I., Picón, A., Acosta, M., Moreno-Fernandez-de-Leceta, A., Garrote, E., and Bereciartua-Perez, A. (2021). MRI Deep Learning-Based Solution for Alzheimer's Disease Prediction, *Journal of Personalized Medicine*, Vol. 11, No. 9, 902. doi:10.3390/jpm11090902.
17. Grzybowski, A., Jin, K., and Wu, H. (2024). Challenges of Artificial Intelligence in Medicine and Dermatology, *Clinics in Dermatology*, Vol. 42, No. 3, 210–215. doi:10.1016/j.clindermatol.2023.12.013.

18. Dwivedi, R., Dave, D., Naik, H., Singhal, S., Omer, R., Patel, P., Qian, B., Wen, Z., Shah, T., Morgan, G., and Ranjan, R. (2023). Explainable AI (XAI): Core Ideas, Techniques, and Solutions, *ACM Computing Surveys*, Vol. 55, No. 9, 1–33. doi:10.1145/3561048.

19. Yakkundi, A. (2023). Alzheimer's Disease Dataset, *Mendeley Data*. doi:10.17632/ch87yswbz4.1.

20. Idroes, G. M., Maulana, A., Suhendra, R., Lala, A., Karma, T., Kusumo, F., Hewindati, Y. T., and Noviandy, T. R. (2023). TeutongNet: A Fine-Tuned Deep Learning Model for Improved Forest Fire Detection, *Leuser Journal of Environmental Studies*, Vol. 1, No. 1, 1–8. doi:10.60084/ljes.v1i1.42.

21. Noviandy, T. R., Idroes, G. M., and Hardi, I. (2024). Machine Learning Approach to Predict AXL Kinase Inhibitor Activity for Cancer Drug Discovery Using XGBoost and Bayesian Optimization, *Journal of Soft Computing and Data Mining*, Vol. 5, No. 1, 46–56.

22. Maulana, A., Noviandy, T. R., Suhendra, R., Earlia, N., Bulqiah, M., Idroes, G. M., Niode, N. J., Sofyan, H., Subianto, M., and Idroes, R. (2023). Evaluation of Atopic Dermatitis Severity Using Artificial Intelligence, *Narra J*, Vol. 3, No. 3, e511. doi:10.52225/narra.v3i3.511.

23. Selvaraju, R. R., Cogswell, M., Das, A., Vedantam, R., Parikh, D., and Batra, D. (2017). Grad-CAM: Visual Explanations from Deep Networks via Gradient-Based Localization, *2017 IEEE International Conference on Computer Vision (ICCV)*, IEEE, 618–626. doi:10.1109/ICCV.2017.74.

24. Idroes, G. M., Noviandy, T. R., Emran, T. Bin, and Idroes, R. (2024). Explainable Deep Learning Approach for Mpox Skin Lesion Detection with Grad-CAM, *Heca Journal of Applied Sciences*, Vol. 2, No. 2, 54–63. doi:10.60084/hjas.v2i2.216.

25. Yang, R., Xiong, X., Wang, H., and Li, W. (2022). Explainable Machine Learning Model to Prediction EGFR Mutation in Lung Cancer, *Frontiers in Oncology*, Vol. 12. doi:10.3389/fonc.2022.924144.

26. Noviandy, T. R., Maulana, A., Zulfikar, T., Rusyana, A., Enitan, S. S., and Idroes, R. (2024). Explainable Artificial Intelligence in Medical Imaging: A Case Study on Enhancing Lung Cancer Detection through CT Images, *Indonesian Journal of Case Reports*, Vol. 2, No. 1, 6–14. doi:10.60084/ijcr.v2i1.150.